Bioconjugate Chemistry

Communication

pubs.acs.org/bc

GLP-1 Receptor Mediated Targeting of a Fluorescent Zn^{2+} Sensor to Beta Cell Surface for Imaging Insulin/Zn^{2+} Release

Daliang Li,[†,#] ZhiJiang Huang,[†] Shiuhwei Chen,[†] Zeping Hu,[‡] and Wen-hong Li*[,†]

[†]Departments of Cell Biology and of Biochemistry, [‡]Children's Medical Center Research Institute, University of Texas Southwestern Medical Center, 6000 Harry Hines Boulevard, Dallas, Texas 75390-9039, United States

Supporting Information

ABSTRACT: The pancreatic islet beta cell plays an essential role in maintaining the normal blood glucose level by releasing insulin. Loss of functional beta cell mass leads to diabetes—a disease affecting ~9% of the population worldwide. There has been great interest and intense effort in developing imaging probes for monitoring islet beta cells, and glucagon-like peptide-1 receptor (GLP-1R) has emerged as a valuable biomarker for targeting beta cells. However, efforts thus far in GLP-1R mediated beta cell labeling and imaging has largely, if not exclusively, focused on developing imaging probes for monitoring beta cell mass, and few studies have investigated imaging beta cell function (insulin release) through GLP-1R. We now report the design and synthesis of a bioconjugate, ZIMIR-Ex4(9−39), that consists of a fluorescent Zn^{2+} sensor and a truncated exendin 4 peptide for imaging insulin/Zn^{2+} release in islet beta cells. In vitro, the conjugate bound to Zn^{2+} with high affinity and displayed a robust fluorescence enhancement upon Zn^{2+} chelation. When added to beta cells at submicromolar concentration, ZIMIR-Ex4(9−39) rapidly labeled cell surface in minutes to report the dynamics of insulin/Zn^{2+} release with high spatiotemporal resolution. Future explorations of this approach may lead to probes for tracking beta cell function using different imaging modalities.

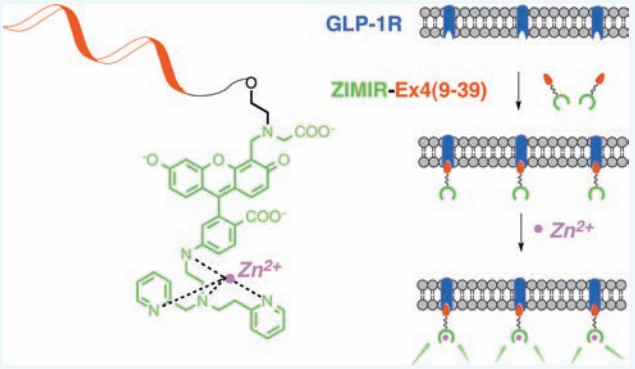

Pancreatic islet beta cells play an essential role in regulating glucose homeostasis by releasing insulin. Impairment of beta cell function causes abnormal insulin secretion that eventually leads to diabetes—a global health problem affecting more than 380 million people worldwide. To better understand the cause and the progression of beta cell injury over the course of diabetes development, there have been significant efforts in developing imaging probes to follow the mass or the function of islet beta cells in vivo.[1] Glucagon-like peptide-1 receptor (GLP-1R) has emerged as a valuable biomarker for beta cell imaging in recent years. In the pancreas, GLP-1R is abundantly expressed in islet beta cells.[2,3] Its native ligand, glucagon-like peptide 1 (GLP-1), binds to GLP-1R with nanomolar affinity. However, since GLP-1 peptide is rapidly degraded by dipeptidyl peptidase in the plasma, it has a very short half-life (~1.5 min) in vivo.[4] Consequently, peptidase resistant GLP-1 analogues have been explored for targeting and imaging of islet beta cells. Exendin-4 (Ex4) is a 39-amino-acid peptide isolated from the lizard Gila monster that binds to GLP-1R with similar affinity as GLP-1.[5] Because Ex4 is much more resistant to peptidase hydrolysis, there has been great interest in developing imaging probes based on Ex4 for monitoring islet beta cells. A variety of labels including ^{111}In,[6,7] ^{99m}Tc,[8] ^{68}Ga,[8,9] ^{64}Cu,[10−12] ^{125}I,[13] ^{18}F,[14−16] superparamagnetic iron oxide nanoparticles,[17] and fluorescent dyes[12,18−20] have been conjugated with Ex4. Combined with different imaging modalities including PET,[8−12,14,16,21,22] SPECT,[8,23,24] MRI,[17] and intravital fluorescent pancreatic laparoscopy,[19] these Ex4-conjugated labels have been utilized to analyze islet beta cells under different settings including live animals, isolated pancreas or islets, and implanted insulinoma cells.

To date, however, efforts in this area have been largely centered around developing Ex4 conjugates for imaging beta cell mass, and there have been few attempts employing GLP-1R as a biomarker to design imaging assays for analyzing beta cell function such as insulin secretion. Exploiting the fact that insulin granules contain a high level of Zn^{2+}, and that Zn^{2+} is co-released with insulin during secretion, we recently developed a fluorescent zinc indicator for monitoring induced exocytotic release (ZIMIR).[25] ZIMIR is an amphipathic molecule containing a pair of lipophilic dodecyl chains (Figure 1A). When added to cells, it rapidly adheres to the plasma membrane through hydrophobic interaction with membrane lipids, and reports local Zn^{2+} elevation near the cell surface.[25] Hence, by using Zn^{2+} efflux as a surrogate marker, we are able to follow the dynamics of insulin secretion with high spatial and temporal resolution in fully intact live cells by digital

Received: May 1, 2015
Published: June 29, 2015

DOI: 10.1021/acs.bioconjchem.5b00332
Bioconjugate Chem. 2015, 26, 1443−1450

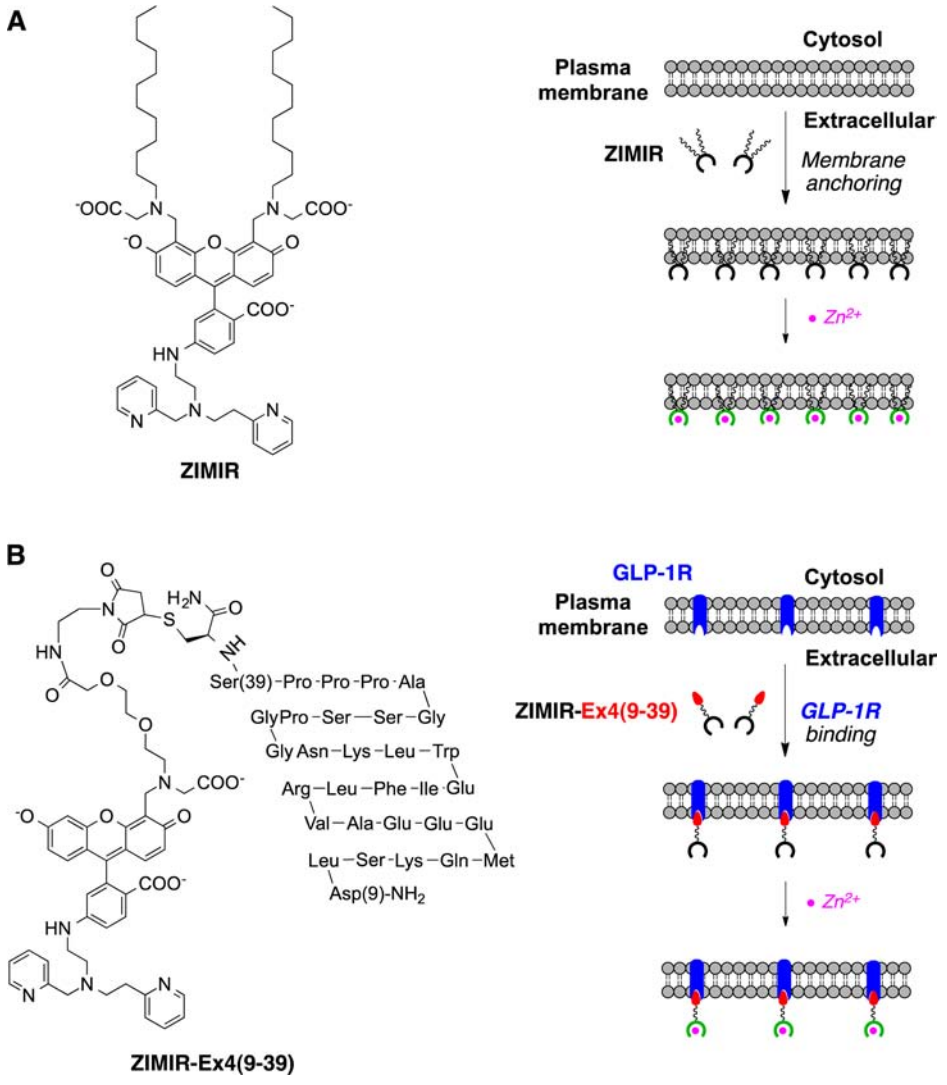

Figure 1. (A) Structure of ZIMIR and its mode of action in membrane labeling and in reporting local Zn^{2+} changes near the outer leaflet of the plasma membrane. Zn^{2+} binding turns on the fluorescence (indicated by the green color) of ZIMIR. (B) ZIMIR-Ex4(9−39) is a peptide conjugate of a hydrophilic Zn^{2+} sensor that labels cell membrane through binding to the GLP-1 receptor on the beta cell surface.

fluorescence microscopy, providing a sensitive and convenient approach to facilitate studying mechanisms regulating stimulus-secretion coupling.[25−27] Zn^{2+} is also known as an obligatory cofactor for forming the dense-core granule in islet beta cells,[28] and zinc transporter 8 (ZnT8, encoded by *SLC30A8* gene) is responsible for Zn^{2+} uptake into insulin granules. Notably, recent genome-wide association studies have uncovered that single-nucleotide polymorphisms (SNPs) in *SLC30A8* gene are associated with altered risk of type 2 diabetes,[29−31] raising the interesting mechanistic questions of how such SNPs affect Zn^{2+} homeostasis, and how the perturbation on Zn^{2+} regulation plays a role in human health or diseases.[32] Once released from islet beta cells, Zn^{2+} can act locally within the islet as an autocrine and/or a paracrine signal.[33] In addition, Zn^{2+} secreted in concert with insulin may exert biological effects on distal tissues or organs through circulation, for example, to suppress hepatic insulin clearance by inhibiting clathrin-dependent insulin endocytosis in the liver.[34] Hence, investigating dynamic Zn^{2+} fluctuation and understanding the regulation of Zn^{2+} homeostasis in live cells represent a significant biomedical challenge with profound implications for human health, and developing new sensing technologies and probes to image Zn^{2+} activity will provide crucial new tools to aid such endeavors.

While cell labeling and imaging with ZIMIR is convenient, rapid, and noninvasive, it nevertheless lacks cell targeting specificity and delivers Zn^{2+} probe to membranes of exposed cells nonselectively. Another strategy is to express an exogeneous protein in cells of interest to enable cell-specific labeling,[35] yet the approach requires the expression of a transgene and hence is applicable primarily to model organisms in which genetic manipulations are feasible. Further, genetic engineering of such model systems can be costly and time-consuming. As a part of our research program to develop new imaging probes for studying stimulus-secretion coupling and Zn^{2+} signaling in pancreatic beta cells, we explored the possibility of targeting endogenous, native cell surface receptors as an alternative strategy for delivering Zn^{2+} probes to cells of interest. In this report, we presented our work developing a bioconjugate containing a fluorescent Zn^{2+} sensor and a truncated Ex4 peptide, Ex4(9−39), for imaging Zn^{2+}/insulin release at the beta cell surface through binding to the GLP-1 receptor (Figure 1B).

DOI: 10.1021/acs.bioconjchem.5b00332
Bioconjugate Chem. 2015, 26, 1443−1450

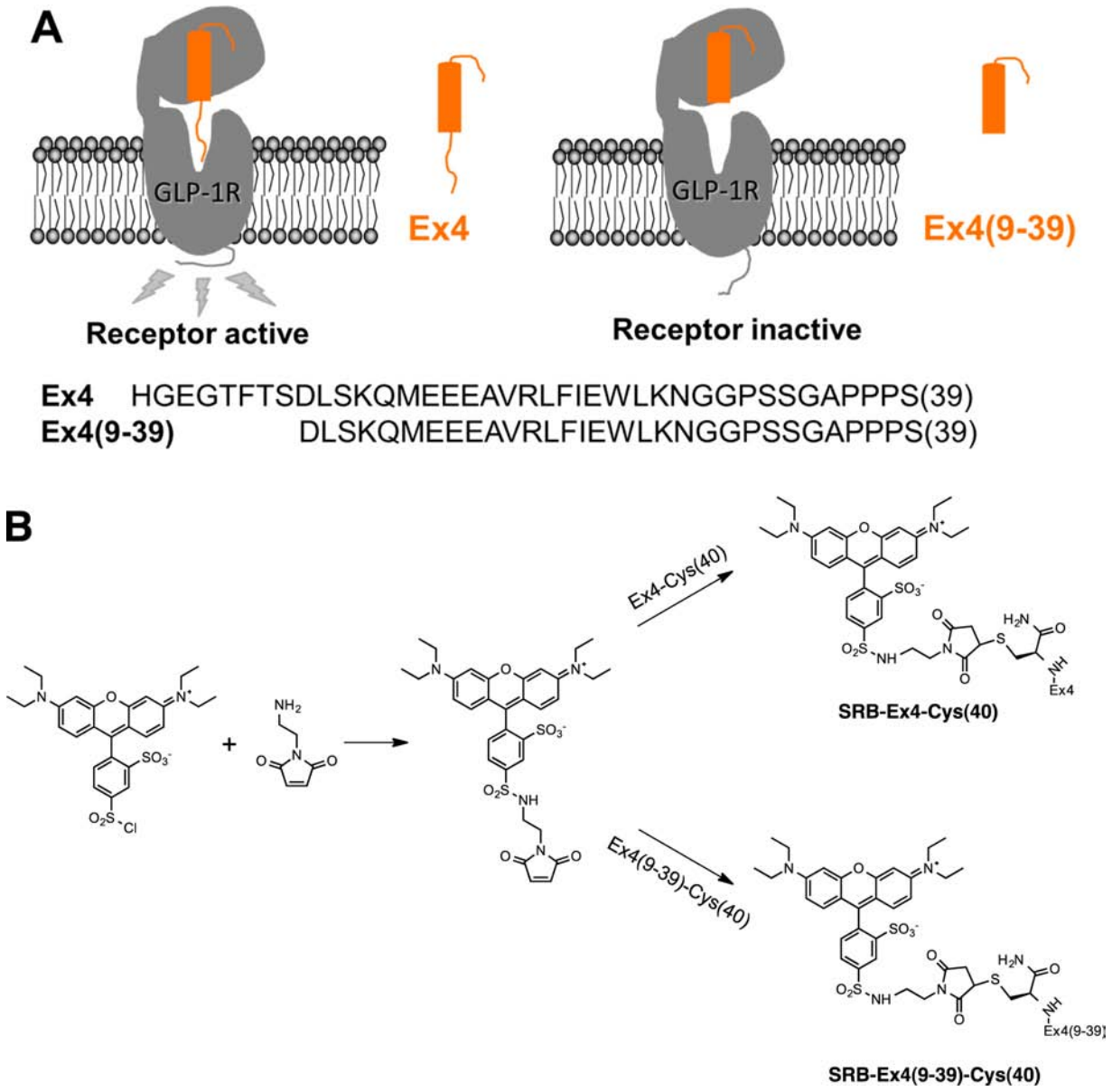

Figure 2. (A) Two-site binding model of GLP-1R with its ligands. The full length Ex4 interacts with both sites to bind to the receptor and to induce receptor activation (left). Ex4(9−39) occupies only the ligand binding domain but not the receptor activation domain. Drawing based on ref 36. Peptide sequences are shown as the standard one letter codes of amino acids. (B) Synthesis of SRB-Ex4-Cys(40) and SRB-Ex4(9−39)-Cys(40).

To select a GLP-1R ligand for conjugating with the fluorescent Zn^{2+} probe, we considered Ex4 and its N-terminal truncated derivative, Ex4(9−39). Previous studies on the structure and activity relationship of the interaction between GLP-1R and its ligands have established a two-site binding model (Figure 2A).[36,37] In this model, the N-terminus of Ex4 interacts with the extracellular surface of the GLP-1R core-domain. This interaction is important for the receptor activation but only makes a minor contribution to the overall binding to the GLP-1R.[36,38,39] The C-terminal helical region of Ex4, on the other hand, interacts with the N-terminal domain of GLP-1R, and this interaction is a major determinant for the high affinity binding between the receptor and its ligands including Ex4 and GLP-1. Hence, a truncated Ex4 analogue, Ex4(9−39), binds to GLP-1R with low nanomolar affinity without inducing receptor activation and hence functions as an antagonist of GLP-1R.

Activating cell surface receptors with their native ligands or agonists normally induces receptor internalization through the process of receptor mediated endocytosis. In contrast, when the truncated ligand Ex4(9−39) was added to cells, GLP-1R was reported to remain on the cell surface after binding to Ex4(9−39).[40] Since we aimed to target Zn^{2+} probes to beta cell surface for imaging insulin/Zn^{2+} release, we reasoned that Ex4(9−39) would be a more appropriate ligand than the full-length Ex4 for the purpose of labeling the cell plasma membrane with the Zn^{2+} sensor. To confirm that Ex4(9−39) conjugated fluorophores resist internalization upon binding to GLP-1R, we labeled full-length Ex4 or truncated Ex4(9−39) with sulforhodamine B maleimide by introducing a cysteine residue at their C-termini (Figure 2B). Previous studies have suggested that the C-terminus of the full-length Ex4 can be extended with additional amino acids without compromising its binding affinity to GLP-1R.[8,11,14−16,18]

DOI: 10.1021/acs.bioconjchem.5b00332
Bioconjugate Chem. 2015, 26, 1443−1450

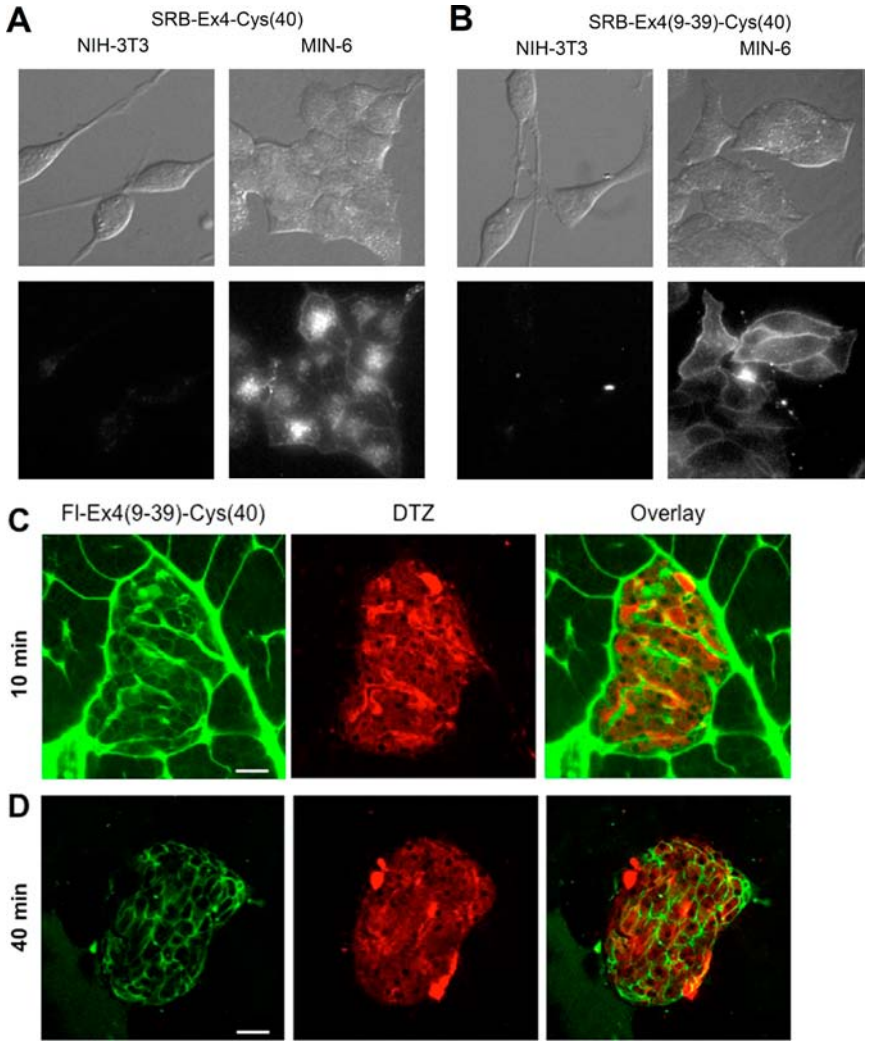

Figure 3. Dye conjugates of Ex4(9−39)-Cys(40), but not of Ex4-Cys(40), accumulated at the cell surface after binding to GLP-1R. (A,B) NIH-3T3 or MIN6 cells were incubated with 100 nM of SRB-Ex4-Cys(40) (A) or SRB-Ex4(9−39)-Cys(40) (B) for 20 min at 37 °C in the secretion assay buffer, washed three times and imaged. DIC and fluorescence images are shown on the top and at the bottom, respectively. (C,D) Fl-Ex4(9−39) selectively accumulated at the beta cell surface in vivo. Fl-Ex4(9−39) (8 nmol/mouse) was injected into anesthetized mice. The mice were sacrificed 10 min (C) or 40 min (D) later, and individual islets (marked by DTZ staining) together with the surrounding exocrine tissue were microdissected from the pancreas and imaged by confocal microscopy.

The resulting conjugates, SRB-Ex4-Cys(40) and SRB-Ex4(9−39)-Cys(40), were tested for their abilities of labeling the cell plasma membrane in cultured MIN6 cells, a beta cell line that abundantly expresses GLP-1R.[41] At 100 nM concentration, SRB-Ex4-Cys(40) was readily taken up by MIN6 cells after 20 min of incubation (Figure 3A). In contrast, little dye uptake was observed in the NIH-3T3 cell, a cell line that does not express GLP-1R.[19] Like SRB-Ex4-Cys(40), SRB-Ex4(9−39)-Cys(40) also selectively labeled MIN6 cells at nanomolar concentration (Figure 3B). However, unlike SRB-Ex4-Cys(40) which showed a predominantly intracellular accumulation through GLP-1R internalization, SRB-Ex4(9−39)-Cys(40) remained on the cell surface with little intracellular uptake. Moreover, we observed no sign of SRB-Ex4(9−39)-Cys(40) internalization even after prolonged incubation up to 3 h (Supporting Information (SI) Figure 1), confirming that the truncated Ex4 peptide would be a suitable ligand for targeting the zinc sensor to the beta cell surface, at least in vitro. To investigate whether Ex4(9−39) conjugates could be used to label the plasma membrane of islet beta cells under the in vivo setting, we prepared fluorescein-Ex4(9−39)-Cys(40) (SI Figure 2A,B, hereinafter referred to as Fl-Ex4(9−39)). Fl-Ex4(9−39) emits green fluorescence so it spectrally complements dithizone (DTZ), a metal chelator that has been shown to mark islet beta cells from its red fluorescence.[42] Combining Fl-Ex4(9−39) with DTZ hence allowed us to perform two-color imaging to track the localization of Fl-Ex4(9−39) with respect to islet beta cells. In addition, a competitive binding assay confirmed that modification of Ex4(9−39) with fluorescein at the C-terminus did not compromise the high binding affinity of the peptide conjugate to GLP-1R (SI Figure 2C), further supporting the feasibility of employing Ex4(9−39) as a targeting moiety to deliver imaging probes to the beta cell surface. After injecting Fl-Ex4(9−39) and DTZ into live mice, we dissected individual islets and their surrounding tissues from the pancreata and examined them under confocal microscopy. Within 10 min following the injection, Fl-Ex4(9−39) was seen in the islets, the blood vessels and, to a lesser extent, the nearby exocrine cells (Figure 3C). By 40 min, however, green fluorescence in the blood vessels and exocrine cells became essentially undetect-

DOI: 10.1021/acs.bioconjchem.5b00332
Bioconjugate Chem. 2015, 26, 1443−1450

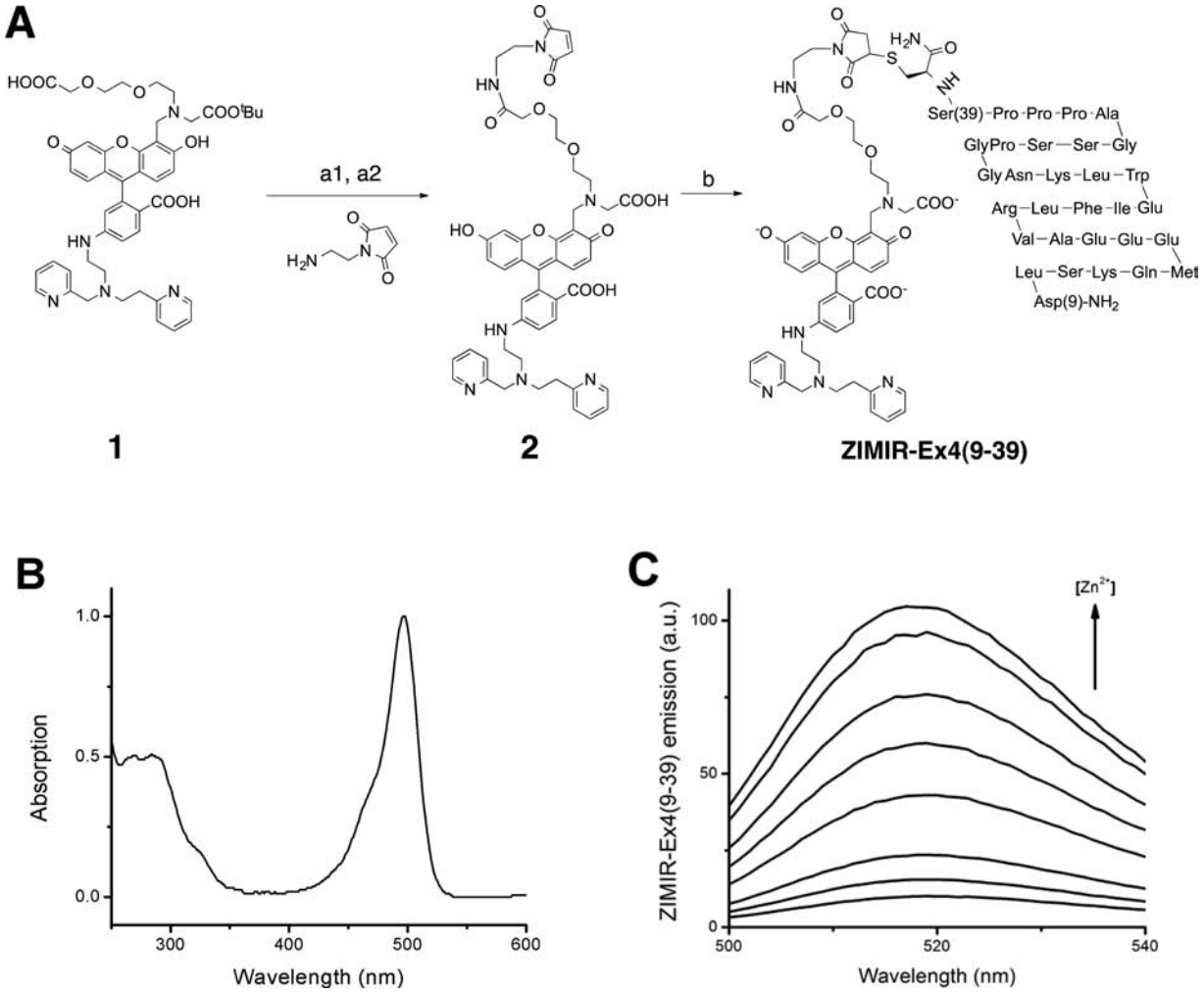

Figure 4. Synthesis and characterization of ZIMIR-Ex4(9−39). (A) Synthesis of ZIMIR-Ex4(9−39). (a1) PyBOP, DMF, RT, overnight, 40%; (a2) TFA, DCM, r.t., 4 h. (b) Ex4(9−39)-Cys(40), 50 mM NaH_2PO_4, 0.15 M NaCl, pH 6.8, DMF, RT, 1 h; then $HSCH_2CH_2OH$, 33%. (B) Absorption spectrum of ZIMIR-Ex4(9−39) in Hank's balanced saline (pH 7.5). The spectrum changed little after adding Zn^{2+}. (C) Zinc titration of ZIMIR-Ex4(9−39) as measured from Zn^{2+} dependent fluorescence enhancement in Hepes buffer (pH 7.5) containing nitrilotriacetic acid. Zn^{2+} concentrations were 0, 10, 25, 443, 843, 1243, 2043, and 3643 nM from the bottom to the top.

able, likely because of the clearance of the injected label from the circulation in vivo. In contrast, pancreatic islets displayed distinct green fluorescence with the surface of the beta cells clearly marked by Fl-Ex4(9−39) (Figure 3D). The result confirmed that truncated Ex4(9−39) should serve as a valuable targeting moiety to deliver fluorescent probes selectively to islet beta cell surface in vivo.

To conjugate Ex4(9−39) with the Zn^{2+} sensor, we designed a ZIMIR analogue by replacing the pair of dodecyl chains of ZIMIR with a single thiol-reactive maleimide group linked to the 4′-position of the xanthene fluorophore (Compound **2**, Figure 4A). This intermediate was prepared from the precursor **1**, synthesized in 10 steps from common starting materials (SI Figure 3). Reaction of maleimide **2** with Ex4(9−39)-Cys(40) under a weakly acidic condition provided the desired peptide conjugate, ZIMIR-Ex4(9−39) (shortened for ZIMIR-Ex4(9−39)-Cys(40)). ZIMIR-Ex4(9−39) absorbed maximally near 490 nm (Figure 4B). In vitro Zn^{2+} titration of ZIMIR-Ex4(9−39) showed a $[Zn^{2+}]$ dependent increase in its fluorescence emission with a submicromolar binding affinity (Figure 4C, $K_d(Zn^{2+}) \approx 0.9$ μM), similar to the binding affinities of other Zn^{2+} chelators containing a mixture of 2-pyridylmethyl and 2-pyridylethyl groups.[25,43] The fluorescence quantum yields of ZIMIR-Ex4(9−39) were determined to be 21% in the Zn^{2+}-bound state and 2% in the Zn^{2+}-free state. Overall, the fluorescence intensity of ZIMIR-Ex4(9−39) enhanced about 10-fold upon Zn^{2+} chelation, confirming that conjugation with Ex4(9−39) peptide did not compromise the Zn^{2+} sensing ability of the ZIMIR derivative. Moreover, fluorescence of ZIMIR-Ex4(9−39) only displayed a minor decrease when changing the pH from 7.2 to 6.4 (SI Figure 4), assuring that a modest acidification near the physiological range should not cause an artificial enhancement of ZIMIR-Ex4(9−39) emission.

To apply ZIMIR-Ex4(9−39) to image Zn^{2+} secretion in live cells, we added 0.1 μM of ZIMIR-Ex4(9−39) to MIN6 cells. Cells were washed 5 min later. Fluorescence imaging revealed green fluorescence along the cell membrane, albeit with low signal intensity in the basal medium as expected (Figure 5A,B). Subsequent stimulation with high KCl (40 mM) depolarized the cell membrane and opened voltage operated calcium channels to allow calcium influx and to activate insulin secretion. Time lapse fluorescence imaging showed a highly dynamic Zn^{2+}/insulin release events along the cell−cell contacts among cells in the filed of view (Figure 5C,E; and

DOI: 10.1021/acs.bioconjchem.5b00332
Bioconjugate Chem. 2015, 26, 1443−1450

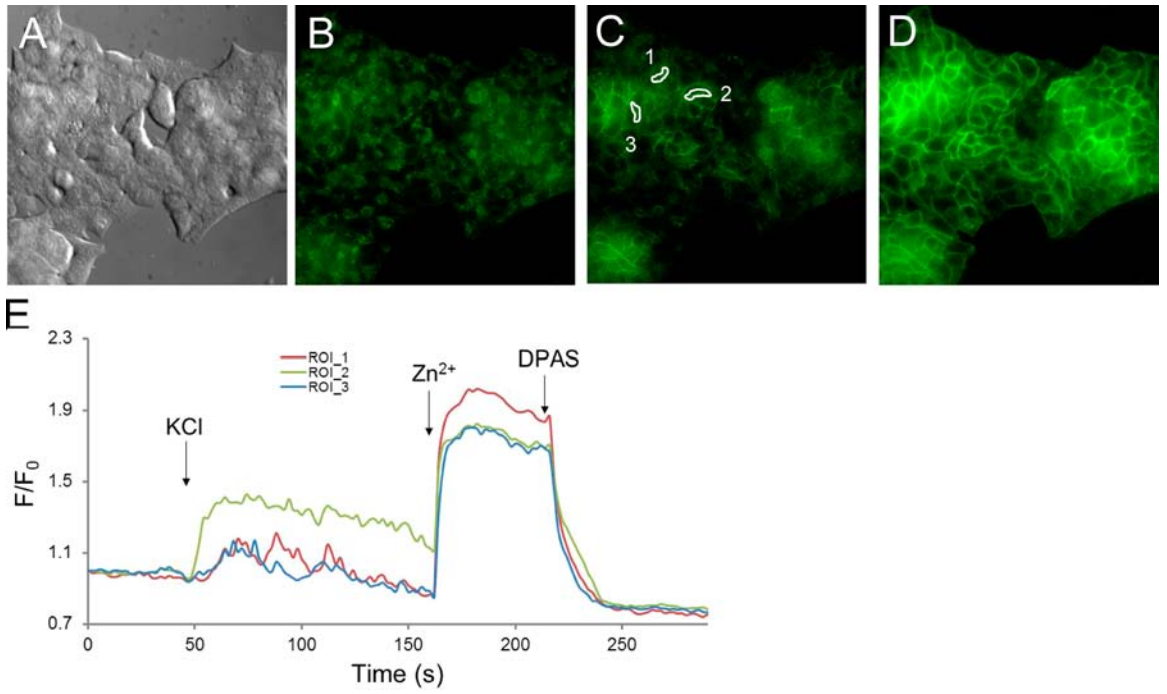

Figure 5. Fluorescence imaging of Zn^{2+}/insulin release in MIN6 cells with ZIMIR-Ex4(9−39). (A−D) Representative cell images (A, DIC; B−D, ZIMIR-Ex4(9−39) fluorescence) before (B) and after (C) KCl (40 mM) stimulation. Zn^{2+} (>1 μM) was added later (D). (E) Time course of membrane ZIMIR-Ex4(9−39) signal of three regions of interest (ROI_1, _2, and _3, outlined in C). DPAS (200 μM) was added at the end to chelate free Zn^{2+}.

SI Movie 1). Later, we added Zn^{2+} to the medium to raise [Zn^{2+}] globally in the bulk solution. This raised ZIMIR-Ex4(9−39) signal in all cells throughout the entire field (Figure 5D,E). Subsequent addition of a fast Zn^{2+} chelator DPAS[25] depleted free Zn^{2+} in the solution and caused ZIMIR-Ex4(9−39) signal to return to the basal level, confirming that Zn^{2+} sensing by ZIMIR-Ex4(9−39) was fully reversible (Figure 5E). The experiment demonstrated that ZIMIR-Ex4(9−39) not only maintained a high binding affinity to GLP-1R to allow rapid labeling of the beta cell membrane, but also was the conjugate effective in reporting local [Zn^{2+}] fluctuations reliably in a cellular environment. To further confirm that ZIMIR-Ex4(9−39) labeled cell surface through GLP-1R, we tested the conjugate in NIH3T3 cells. Even at 1 μM concentration and after prolonged incubation (>30 min), we did not observe any membrane staining of ZIMIR-Ex4(9−39) in NIH3T3 cells bathed either in the basal medium or in a medium containing high Zn^{2+} (data not shown). Moreover, in MIN6 cells, addition of Ex4 peptide to the dye loading solution prevented ZIMIR-Ex4(9−39) from labeling the cell membrane (SI Figure 5), demonstrating the specific cellular uptake of ZIMIR-Ex4(9−39) through GLP-1R.

Finally, to further confirm that the cell internalization of the full-length Ex4 is a general phenomenon that occurs regardless of the cargo to which it is conjugated, we prepared ZIMIR-Ex4 following the same procedure as making ZIMIR-Ex4(9−39) (SI Figure 6A). In the cuvette, ZIMIR-Ex4 behaved similarly to ZIMIR-Ex4(9−39) and displayed [Zn^{2+}]-dependent fluorescence enhancement (SI Figure 6B). Its fluorescence intensity increased 18-fold upon Zn^{2+} chelation. However, when ZIMIR-Ex4 was added to cells, it was quickly internalized into cells as revealed by fluorescence imaging, and the probe barely showed any response when Zn^{2+} (μM) was added to the extracellular medium (SI Figure 7), which was in striking contrast to the large response reported by ZIMIR-Ex4(9−39) (Figure 5D,E). Combining our previous observation on the rapid cellular uptake of SRB-Ex4 (Figure 3A) with reports from others,[40] we concluded that GLP-1R mediated internalization of Ex4-dye conjugates appeared to be a general and facile process regardless which fluorophores were used.

In summary, exploiting GLP-1R as a beta cell specific biomarker, we have developed a peptide conjugate of a fluorescent zinc sensor for the functional imaging of islet beta cells. Previous works in this area have been focused on using the full-length Ex4 as the targeting moiety, with the goal of generating probes for imaging beta cell mass. In contrast, our work reported here illustrated the feasibility of targeting GLP-1R to perform functional imaging (insulin secretion) of islet beta cells. We speculate that the strategy presented in this work of using truncated exendin 4 peptide to restrict the labeling of beta cells to the plasma membrane may be of general utility for designing additional probes for monitoring other biochemical events that occur locally at the cell surface. Besides fluorescence microscopy, other whole body imaging modalities such as magnetic resonance imaging (MRI) have been explored for tracking pancreatic beta cell function such as Zn^{2+} secretion in live animals.[44,45] How to integrate those magnetic sensors with the cell surface targeting strategy presented here raises interesting possibilities and challenges for the future engineering of imaging probes for the functional analysis of islet beta cells in vivo.

■ ASSOCIATED CONTENT

Supporting Information

Supplementary figures and a movie, and Methods for synthesis, in vitro characterization, and live cell imaging. The Supporting Information is available free of charge on the ACS Publications website at DOI: 10.1021/acs.bioconjchem.5b00332.

DOI: 10.1021/acs.bioconjchem.5b00332
Bioconjugate Chem. 2015, 26, 1443−1450

AUTHOR INFORMATION

Corresponding Author

*E-mail: Wen-hong.li@utsouthwestern.edu. Tel: (214) 648-3879. Fax: (214) 648-5814.

Present Address

[#]Center for Biomedical Research of South China and College of Life Science, Fujian Normal University, Fujian, 350117, China

Notes

The authors declare no competing financial interest.

ACKNOWLEDGMENTS

This work was supported by National Institutes of Health grant R01 GM077593 and Juvenile Diabetes Research Foundation grant 17-2013-494.

REFERENCES

(1) Gotthardt, M., Eizirik, D. L., Cnop, M., and Brom, M. (2014) Beta cell imaging - a key tool in optimized diabetes prevention and treatment. *Trends Endocrinol. Metab. 25*, 375−377.

(2) Tornehave, D., Kristensen, P., Romer, J., Knudsen, L. B., and Heller, R. S. (2008) Expression of the GLP-1 receptor in mouse, rat, and human pancreas. *J. Histochem. Cytochem. 56*, 841−851.

(3) Holst, J. J. (2007) The physiology of glucagon-like peptide 1. *Physiol. Rev. 87*, 1409−1439.

(4) Vilsboll, T., Agerso, H., Krarup, T., and Holst, J. J. (2003) Similar elimination rates of glucagon-like peptide-1 in obese type 2 diabetic patients and healthy subjects. *J. Clin. Endocrinol. Metab. 88*, 220−224.

(5) Goke, R., Fehmann, H. C., Linn, T., Schmidt, H., Krause, M., Eng, J., and Goke, B. (1993) Exendin-4 is a high potency agonist and truncated exendin-(9−39)-amide an antagonist at the glucagon-like peptide 1-(7−36)-amide receptor of insulin-secreting beta-cells. *J. Biol. Chem. 268*, 19650−19655.

(6) Wild, D., Behe, M., Wicki, A., Storch, D., Waser, B., Gotthardt, M., Keil, B., Christofori, G., Reubi, J. C., and Macke, H. R. (2006) [Lys40(Ahx-DTPA-111In)NH2]exendin-4, a very promising ligand for glucagon-like peptide-1 (GLP-1) receptor targeting. *J. Nucl. Med. 47*, 2025−2033.

(7) Christ, E., Wild, D., Forrer, F., Brandle, M., Sahli, R., Clerici, T., Gloor, B., Martius, F., Maecke, H., and Reubi, J. C. (2009) Glucagon-like peptide-1 receptor imaging for localization of insulinomas. *J. Clin. Endocrinol. Metab. 94*, 4398−4405.

(8) Wild, D., Wicki, A., Mansi, R., Behe, M., Keil, B., Bernhardt, P., Christofori, G., Ell, P. J., and Macke, H. R. (2010) Exendin-4-based radiopharmaceuticals for glucagonlike peptide-1 receptor PET/CT and SPECT/CT. *J. Nucl. Med. 51*, 1059−1067.

(9) Selvaraju, R. K., Velikyan, I., Johansson, L., Wu, Z., Todorov, I., Shively, J., Kandeel, F., Korsgren, O., and Eriksson, O. (2013) In vivo imaging of the glucagonlike peptide 1 receptor in the pancreas with 68Ga-labeled DO3A-exendin-4. *J. Nucl. Med. 54*, 1458−1463.

(10) Wu, Z., Liu, S., Nair, I., Omori, K., Scott, S., Todorov, I., Shively, J. E., Conti, P. S., Li, Z., and Kandeel, F. (2014) (64)Cu Labeled Sarcophagine Exendin-4 for MicroPET Imaging of Glucagon like Peptide-1 Receptor Expression. *Theranostics 4*, 770−777.

(11) Wu, Z., Todorov, I., Li, L., Bading, J. R., Li, Z., Nair, I., Ishiyama, K., Colcher, D., Conti, P. E., Fraser, S. E., et al. (2011) In Vivo Imaging of Transplanted Islets with (64)Cu-DO3A-VS-Cys(40)-Exendin-4 by Targeting GLP-1 Receptor. *Bioconjugate Chem. 22*, 1587−1594.

(12) Brand, C., Abdel-Atti, D., Zhang, Y., Carlin, S., Clardy, S. M., Keliher, E. J., Weber, W. A., Lewis, J. S., and Reiner, T. (2014) In Vivo Imaging of GLP-1R with a Targeted Bimodal PET/Fluorescence Imaging Agent. *Bioconjugate Chem. 25*, 1323−1330.

(13) Mukai, E., Toyoda, K., Kimura, H., Kawashima, H., Fujimoto, H., Ueda, M., Temma, T., Hirao, K., Nagakawa, K., Saji, H., et al. (2009) GLP-1 receptor antagonist as a potential probe for pancreatic beta-cell imaging. *Biochem. Biophys. Res. Commun. 389*, 523−526.

(14) Kiesewetter, D. O., Guo, N., Guo, J., Gao, H., Zhu, L., Ma, Y., Niu, G., and Chen, X. (2012) Evaluation of an [(18)F]AlF-NOTA Analog of Exendin-4 for Imaging of GLP-1 Receptor in Insulinoma. *Theranostics 2*, 999−1009.

(15) Yue, X., Kiesewetter, D. O., Guo, J., Sun, Z., Zhang, X., Zhu, L., Niu, G., Ma, Y., Lang, L., and Chen, X. (2013) Development of a new thiol site-specific prosthetic group and its conjugation with [Cys(40)]-exendin-4 for in vivo targeting of insulinomas. *Bioconjugate Chem. 24*, 1191−1200.

(16) Wu, Z., Liu, S., Hassink, M., Nair, I., Park, R., Li, L., Todorov, I., Fox, J. M., Li, Z., Shively, J. E., et al. (2013) Development and evaluation of 18F-TTCO-Cys40-Exendin-4: a PET probe for imaging transplanted islets. *J. Nucl. Med. 54*, 244−251.

(17) Wang, P., Yoo, B., Yang, J., Zhang, X., Ross, A., Pantazopoulos, P., Dai, G., and Moore, A. (2014) GLP-1R-targeting magnetic nanoparticles for pancreatic islet imaging. *Diabetes 63*, 1465−1474.

(18) Reiner, T., Kohler, R. H., Liew, C. W., Hill, J. A., Gaglia, J., Kulkarni, R. N., and Weissleder, R. (2010) Near-infrared fluorescent probe for imaging of pancreatic beta cells. *Bioconjugate Chem. 21*, 1362−1368.

(19) Reiner, T., Thurber, G., Gaglia, J., Vinegoni, C., Liew, C. W., Upadhyay, R., Kohler, R. H., Li, L., Kulkarni, R. N., Benoist, C., et al. (2011) Accurate measurement of pancreatic islet {beta}-cell mass using a second-generation fluorescent exendin-4 analog. *Proc. Natl. Acad. Sci. U. S. A. 108*, 12815−12820.

(20) Clardy, S. M., Keliher, E. J., Mohan, J. F., Sebas, M., Benoist, C., Mathis, D., and Weissleder, R. (2014) Fluorescent Exendin-4 Derivatives for Pancreatic beta-Cell Analysis. *Bioconjugate Chem. 25*, 171−177.

(21) Brom, M., Oyen, W. J., Joosten, L., Gotthardt, M., and Boerman, O. C. (2010) 68Ga-labelled exendin-3, a new agent for the detection of insulinomas with PET. *Eur. J. Nucl. Med. Mol. Imaging 37*, 1345−1355.

(22) Kiesewetter, D. O., Gao, H., Ma, Y., Niu, G., Quan, Q., Guo, N., and Chen, X. (2012) 18F-radiolabeled analogs of exendin-4 for PET imaging of GLP-1 in insulinoma. *Eur. J. Nucl. Med. Mol. Imaging 39*, 463−473.

(23) Gotthardt, M., Lalyko, G., van Eerd-Vismale, J., Keil, B., Schurrat, T., Hower, M., Laverman, P., Behr, T. M., Boerman, O. C., Goke, B., et al. (2006) A new technique for in vivo imaging of specific GLP-1 binding sites: first results in small rodents. *Regul. Pept. 137*, 162−167.

(24) Brom, M., Woliner-van der Weg, W., Joosten, L., Frielink, C., Bouckenooghe, T., Rijken, P., Andralojc, K., Goke, B. J., de Jong, M., Eizirik, D. L., et al. (2014) Non-invasive quantification of the beta cell mass by SPECT with (111)In-labelled exendin. *Diabetologia 57*, 950−959.

(25) Li, D., Chen, S., Bellomo, E. A., Tarasov, A. I., Kaut, C., Rutter, G. A., and Li, W. H. (2011) Imaging dynamic insulin release using a fluorescent zinc indicator for monitoring induced exocytotic release (ZIMIR). *Proc. Natl. Acad. Sci. U. S. A. 108*, 21063−21068.

(26) Hodson, D. J., Mitchell, R. K., Bellomo, E. A., Sun, G., Vinet, L., Meda, P., Li, D., Li, W. H., Bugliani, M., Marchetti, P., et al. (2013) Lipotoxicity disrupts incretin-regulated human beta cell connectivity. *J. Clin. Invest. 123*, 4182−4194.

(27) Hodson, D. J., Mitchell, R. K., Marselli, L., Pullen, T. J., Brias, S. G., Semplici, F., Everett, K. L., Cooper, D. M., Bugliani, M., Marchetti, P., et al. (2014) ADCY5 couples glucose to insulin secretion in human islets. *Diabetes 63*, 3009−3021.

(28) Dodson, G., and Steiner, D. (1998) The role of assembly in insulin's biosynthesis. *Curr. Opin. Struct. Biol. 8*, 189−194.

(29) Flannick, J., Thorleifsson, G., Beer, N. L., Jacobs, S. B., Grarup, N., Burtt, N. P., Mahajan, A., Fuchsberger, C., Atzmon, G., Benediktsson, R., et al. (2014) Loss-of-function mutations in SLC30A8 protect against type 2 diabetes. *Nat. Genet. 46*, 357.

(30) Davidson, H. W., Wenzlau, J. M., and O'Brien, R. M. (2014) Zinc transporter 8 (ZnT8) and beta cell function. *Trends Endocrinol. Metab. 25*, 415−424.

(31) Rutter, G. A., and Chimienti, F. (2015) SLC30A8 mutations in type 2 diabetes. *Diabetologia 58*, 31−36.

DOI: 10.1021/acs.bioconjchem.5b00332
Bioconjugate Chem. 2015, 26, 1443−1450

(32) Kambe, T., Hashimoto, A., and Fujimoto, S. (2014) Current understanding of ZIP and ZnT zinc transporters in human health and diseases. *Cell. Mol. Life Sci. 71*, 3281−3295.
(33) Chimienti, F. (2013) Zinc, pancreatic islet cell function and diabetes: new insights into an old story. *Nutr. Res. Rev. 26*, 1−11.
(34) Tamaki, M., Fujitani, Y., Hara, A., Uchida, T., Tamura, Y., Takeno, K., Kawaguchi, M., Watanabe, T., Ogihara, T., Fukunaka, A., et al. (2013) The diabetes-susceptible gene SLC30A8/ZnT8 regulates hepatic insulin clearance. *J. Clin. Invest. 123*, 4513−4524.
(35) Li, D., Liu, L., and Li, W. H. (2015) Genetic Targeting of a Small Fluorescent Zinc Indicator to Cell Surface for Monitoring Zinc Secretion. *ACS Chem. Biol. 10*, 1054−1063.
(36) Al-Sabah, S., and Donnelly, D. (2003) A model for receptor-peptide binding at the glucagon-like peptide-1 (GLP-1) receptor through the analysis of truncated ligands and receptors. *Br. J. Pharmacol. 140*, 339−346.
(37) Neumann, J. M., Couvineau, A., Murail, S., Lacapere, J. J., Jamin, N., and Laburthe, M. (2008) Class-B GPCR activation: is ligand helix-capping the key? *Trends Biochem. Sci. 33*, 314−319.
(38) Hoare, S. R. (2005) Mechanisms of peptide and nonpeptide ligand binding to Class B G-protein-coupled receptors. *Drug Discovery Today 10*, 417−427.
(39) Kirkpatrick, A., Heo, J., Abrol, R., and Goddard, W. A., 3rd. (2012) Predicted structure of agonist-bound glucagon-like peptide 1 receptor, a class B G protein-coupled receptor. *Proc. Natl. Acad. Sci. U. S. A. 109*, 19988−19993.
(40) Widmann, C., Dolci, W., and Thorens, B. (1995) Agonist-induced internalization and recycling of the glucagon-like peptide-1 receptor in transfected fibroblasts and in insulinomas. *Biochem. J. 310* (Pt 1), 203−214.
(41) Yamato, E., Ikegami, H., Takekawa, K., Fujisawa, T., Nakagawa, Y., Hamada, Y., Ueda, H., and Ogihara, T. (1997) Tissue-specific and glucose-dependent expression of receptor genes for glucagon and glucagon-like peptide-1 (GLP-1). *Horm. Metab. Res. 29*, 56−59.
(42) Jiao, L., Gray, D. W., Gohde, W., Flynn, G. J., and Morris, P. J. (1991) In vitro staining of islets of Langerhans for fluorescence-activated cell sorting. *Transplantation 52*, 450−452.
(43) Komatsu, K., Kikuchi, K., Kojima, H., Urano, Y., and Nagano, T. (2005) Selective zinc sensor molecules with various affinities for Zn2+, revealing dynamics and regional distribution of synaptically released Zn2+ in hippocampal slices. *J. Am. Chem. Soc. 127*, 10197−10204.
(44) Lubag, A. J., De Leon-Rodriguez, L. M., Burgess, S. C., and Sherry, A. D. (2011) Noninvasive MRI of beta-cell function using a Zn2+-responsive contrast agent. *Proc. Natl. Acad. Sci. U. S. A. 108*, 18400−18405.
(45) Li, W. H., and Li, D. (2013) Fluorescent probes for monitoring regulated secretion. *Curr. Opin. Chem. Biol. 17*, 672−681.

DOI: 10.1021/acs.bioconjchem.5b00332
Bioconjugate Chem. 2015, 26, 1443−1450